Experimental Brain Research (2019) 237:57–70
https://doi.org/10.1007/s00221-018-5395-z

RESEARCH ARTICLE

Looking up while reaching out: the neural correlates of making eye and arm movements in different spatial planes

Diana J. Gorbet[1,2] · **Lauren E. Sergio**[1,2]

Received: 4 July 2018 / Accepted: 4 October 2018 / Published online: 10 October 2018

Abstract

Standard visually guided reaching begins with foveation of a target of interest followed by an arm movement to the same spatial location. However, many visually guided arm movements, as well as a majority of imaging studies examining such movements, require participants to perform non-standard visuomotor mappings where the locations of gaze and arm movements are spatially dissociated (e.g. gaze fixation peripheral to the target of a reaching movement, or use of a tool such as a joystick while viewing stimuli on a screen). In this study, we compare brain activity associated with the production of standard visually guided arm movements to activity during a visuomotor mapping where saccades and reaches were made in different spatial planes. Multi-voxel pattern analysis revealed that while spatial patterns of voxel activity remain quite similar for the two visuomotor mappings during presentation of a cue for movement, patterns of activity become increasingly more discriminative throughout the brain as planning progresses toward motor execution. Decoding of the visuomotor mappings occurs throughout visuomotor-related regions of the brain including the premotor, primary motor and somatosensory, posterior parietal, middle occipital, and medial occipital cortices, and in the cerebellum. These results show that relative to standard visuomotor tasks, activity differs substantially in areas throughout the brain when a task requires an implicit sensorimotor recalibration.

Keywords Eye–hand coordination · Sensory-motor mapping · fMRI · Cognitive-motor integration · Visuomotor control

Introduction

During "standard" visually guided reaching, a saccade and an arm movement are made to the same location in space. In contrast, some visually guided reaching tasks require gaze to be spatially decoupled from an arm movement. A common example includes movement of a computer mouse on a horizontal plane to control a cursor viewed on a vertical screen. Tasks that decouple the guiding visual information from the spatial location of effector movement are referred to as "non-standard" visuomotor mappings (Wise et al. 1996; Gorbet et al. 2004).

Neural signals associated with control of the eyes and arm overlap in many regions of the brain. For example, parietal neurons considered to be primarily involved in planning reaching movements may encode arm movement in an eye-centred reference frame (Batista et al. 1999; Snyder et al. 2000; Cohen and Andersen 2002; Crawford et al. 2004; Buneo et al. 2008). Similarly, arm movements also influence neural activity in regions generally considered to be eye movement control areas (Mushiake et al. 1996; Reyes-Puerta et al. 2010). Further evidence that the eyes and arm share neural resources comes from adaptation experiments that demonstrate transfer from one effector to the other (Kröller et al. 1999; Grigorova et al. 2013). In addition, studies using a variety of psychophysical approaches demonstrate mutually influential effects of the eyes and arm on each other (Fisk and Goodale 1985; Neggers and Bekkering 2000; Lee et al. 2014). It is perhaps not surprising that control of the eyes and arm are linked in the brain since stabilizing gaze at the location of the target of an ongoing reach results in more accurate arm movements (Prablanc et al. 1979). This neural coupling also makes sense from an evolutionary perspective since non-standard visuomotor mappings are relatively rare in natural settings, and avoiding the need to independently

✉ Diana J. Gorbet
gorbetd@yorku.ca

[1] School of Kinesiology and Health Science, York University, Toronto, ON, Canada

[2] Centre for Vision Research, York University, Toronto, ON, Canada

plan reaches and eye movements decreases the amount of processing needed to control visually guided movements. To perform a non-standard visuomotor mapping, inhibition of this putative functional network coupling reach and gaze might be necessary (Carey et al. 1997; Gorbet et al. 2004).

In addition to possibly having to inhibit the default coupling of the eyes and arm, non-standard movements may also require cognitive–motor integration. Explicit, task-relevant rules must often be incorporated into reach planning. For example, move the computer mouse forward to move the cursor upward on the screen. Or, press the brake pedal at red traffic lights and the accelerator pedal at green lights. Beyond the incorporation of sets of explicit rules, implicit sensorimotor recalibration is required during non-standard mappings to account for the decoupling of the guiding visual information from the proprioceptive and motoric components of the task. In the computer mouse example, rather than touching the cursor on the vertical plane of the screen, the arm must make movements along a horizontal plane. Proprioceptive feedback from the arm and patterns of necessary muscle activation are no longer congruent with a standard mapping to the spatial location from which visual guidance is obtained. Further, non-standard tasks can change the relationship between the gain of visual feedback relative to the distance moved by the arm (for example, small movements of the arm controlling a computer mouse may move the cursor large distances on the screen). These altered spatial relationships require internal recalibration for successful performance of non-standard visuomotor mappings (Redding and Wallace 1993; Henriques and Cressman 2012; Granek and Sergio 2015). Previously we have shown that regions in both the dorsal premotor cortex and superior parietal cortex alter both the single-unit and local field potential activity when reaching on a horizontal plane while viewing the guiding visual stimuli on a frontal plane, relative to standard reaching (Hawkins et al. 2013; Sayegh et al. 2013, 2014, 2017). These non-human primate findings provide insight into which components of the parieto-frontal network for reach control may be important for decoupling the actions of the eye and the limb for goal-directed behaviour.

The ability to successfully perform non-standard tasks is impaired in some patient populations even when the production of standard movements remains intact. For example, deficits in the production of non-standard movements are observable in patients diagnosed with mild cognitive impairment (Salek et al. 2011), dementia (Tippett and Sergio 2006; Tippett et al. 2012), and in individuals who are at a higher risk for future dementia (due to a family history or the presence of genetic markers) even in the absence of observable cognitive deficits (Hawkins and Sergio 2014; Hawkins et al. 2015). Importantly, in these populations, standard visually guided movements remain indistinguishable from movements made by healthy control participants. Similarly, athletes with a history of concussion who have passed clinical screening and are considered asymptomatic can also demonstrate detectable deficits in non-standard visuomotor mapping production without any observable problems with standard movements (Brown et al. 2015; Dalecki et al. 2016; Hurtubise et al. 2016). In addition, difficulty specific to non-standard visually guided movements is observed in individuals with non-foveal optic ataxia where reaches to non-foveated targets are grossly inaccurate (Buxbaum and Coslett 1997; Granek et al. 2013; Granek and Sergio 2015) or in dramatic cases, not possible at all (Carey et al. 1997). Similar deficits in non-standard movement production have been documented after damage to the cerebellum (Frassinetti et al. 2007). Finally, the nature of deficits in non-standard visuomotor mapping execution appear to depend on what type of damage the brain has suffered (Hawkins and Sergio 2014; Brown et al. 2015). A greater understanding of the neural correlates of the different components of non-standard movement production in humans (i.e. inhibition of putative circuitry coupling the eyes and arm, explicit rule incorporation, and implicit sensorimotor recalibration) could ultimately provide insight into brain structures at risk in specific patient populations.

The sensorimotor adaptation required when learning a novel non-standard visuomotor mapping is thought to rely upon at least two distinct neurological processes; one that progresses with a relatively fast time-course and that responds strongly to errors and one that progresses relatively more slowly, is less sensitive to errors, and persists for a longer period of time (Smith et al. 2006). Others have shown that the observed fast component of learning corresponds well with the explicit component of sensorimotor adaptation and the slow component corresponds with the implicit aspects of sensorimotor adaptation (Taylor et al. 2014; McDougle et al. 2015). Further, the explicit aspect of sensorimotor adaptation demonstrates greater generalization than that of the implicit component of tasks (Heuer and Hegele 2011). Also, explicit strategic control has been observed to decline with age but implicit recalibration remains intact (McNay and Willingham 1998; Bock and Girgenrath 2006). Indeed, the explicit and implicit aspects of movement control in non-standard visuomotor mapping are differentially susceptible to interference (Granek and Sergio 2015) and are not affected equally in cases of optic ataxia (Granek et al. 2013). These observations all suggest the presence of distinct neurological substrates for the explicit and implicit aspects of non-standard visuomotor performance.

Neuroimaging studies that examine truly standard visuomotor mapping where eye and arm movements are made to the same spatial location are rare. Studies of visuomotor control usually rely upon tool-like interfaces (e.g. joysticks and button boxes) that control a cursor, which is sometimes even viewed indirectly via a mirror. These studies also often

require participants to fixate their gaze during arm responses which is by definition, a non-standard task. Therefore, there are very few direct comparisons of the neural correlates of standard versus non-standard visuomotor control in humans (Gorbet et al. 2004; Gorbet and Sergio 2007, 2016; Granek et al. 2010). In a recent study, we used functional MRI to examine a task in which participants spatially dissociated eye and arm movements using an explicit rule describing a visuomotor rotation. Specifically, participants made a saccadic eye movement to a visually cued target location but moved the arm 180° in the opposite direction (Gorbet and Sergio 2016). Compared with a standard mapping (i.e. eyes and arm both to the visually cued target), the non-standard task was associated with higher activity in the right inferior parietal lobule and a region of the left posterior lobe of the cerebellum. In addition, multi-voxel pattern analysis revealed significant discrimination of the standard versus non-standard mappings bilaterally in the medial premotor cortex and cuneus. The non-standard visuomotor task in this previous study required integration of an explicit rule (i.e. move the arm in the opposite direction of the target). The purpose of the current study is to examine brain activity specifically associated with the implicit aspects of sensorimotor recalibration in non-standard visuomotor control. Using fMRI, we compared brain activity during standard visuomotor mapping with activity during a non-standard mapping that required participants to make movements that were kinematically similar to the standard mapping but in a different spatial plane than the guiding visual information. To our knowledge this is the first comparison of the neural correlates of sensorimotor recalibration to standard visuomotor mapping in humans. Here we present a network of brain regions that, over the course of movement preparation and execution, increasingly discriminate between standard visuomotor mapping and a non-standard task requiring implicit sensorimotor recalibration.

Methods

Participants

Participants of the study were 10 women (mean age 28.4 ± SD 10.6 years). Due to limitations on the number of participants that could be included in the study, only women were included to control for known sex-related differences in the neural control of visually guided arm movements (Gorbet and Sergio 2007; Gorbet et al. 2010; Gorbet and Staines 2011). All participants had normal or corrected-to-normal vision and were right-handed. None of the participants had any known neurological problems. The experimental protocol was approved by the York University Research Ethics Board human participants subcommittee and all participants provided informed written consent before data collection. The experimental protocol was also in compliance with the Declaration of Helsinki.

Apparatus

A 3T Siemens Magnetom Avanto MRI system located at York University was used for MRI data acquisition. Participants lay in a supine position in the scanner with their heads tilted forward approximately 30° using a plastic wedge placed under the head coil. This position allowed participants to directly view stimuli that were back-projected onto a vertical plastic screen at a resolution of 1024 × 768 with a refresh interval of 60 Hz. A transparent touchpad measuring 17.00 cm × 12.8 cm (Keytec Inc. Garland, Texas, USA) was mounted to the vertical plastic screen. A second touchpad (also with an active area measuring 17.00 cm × 12.8 cm) was located in front of the vertical screen in a horizontal position (Fig. 1). The screen apparatus was fixed to the scanner bed in a position that allowed participants to slide their finger to projected targets using small movements of the wrist and lower arm on either the vertical or horizontal touchpad. Lighting in the MRI suite was kept dim to allow optimal viewing of the projected stimuli while still allowing participants to see their own hand moving on the touchpads.

Tilting participants' heads for direct viewing of targets for movement required the use of the bottom half of a 12-channel receive-only head coil at the back of the head (integrated into the head cradle) with a 4-channel flex coil over the forehead to collect signal from the anterior part of the brain (Chen et al. 2014; Gorbet and Sergio 2016). Foam padding was used to secure participants' heads in place. To minimize head movement resulting from motion of the arm, participants' right upper arms were secured in place using a velcro strap and padding.

T1-weighted anatomical image collection used 192 slices in the sagittal orientation, TR = 2300 ms, TE = 2.62 ms, flip angle = 9°, FoV = 256 mm, and voxel dimension of 1.0 × 1.0 × 1.0 mm. Functional images covered the entire brain and cerebellum using T2*-weighted gradient echoplanar imaging with TR = 3000 ms, TE = 30 ms, flip angle = 90°, FoV = 240 mm. Forty-nine, 3.0-mm thick slices with a voxel dimension of 3.0 × 3.0 × 3.0 mm were collected with an interleaved acquisition sequence and zero gap between slices.

Movements of the right eye were monitored using an MRI-compatible eye tracker system (Avotec Eye Tracking System RE-5721, Stuart, FL; sampling rate of 60 Hz, spatial resolution of 0.1° of eye movement). However, the tilting of participants' heads made it difficult to position the eye tracker camera for ideal tracking without blocking the view of targets projected onto the screen. Therefore, eye position data were often intermittent due to the camera's view of the

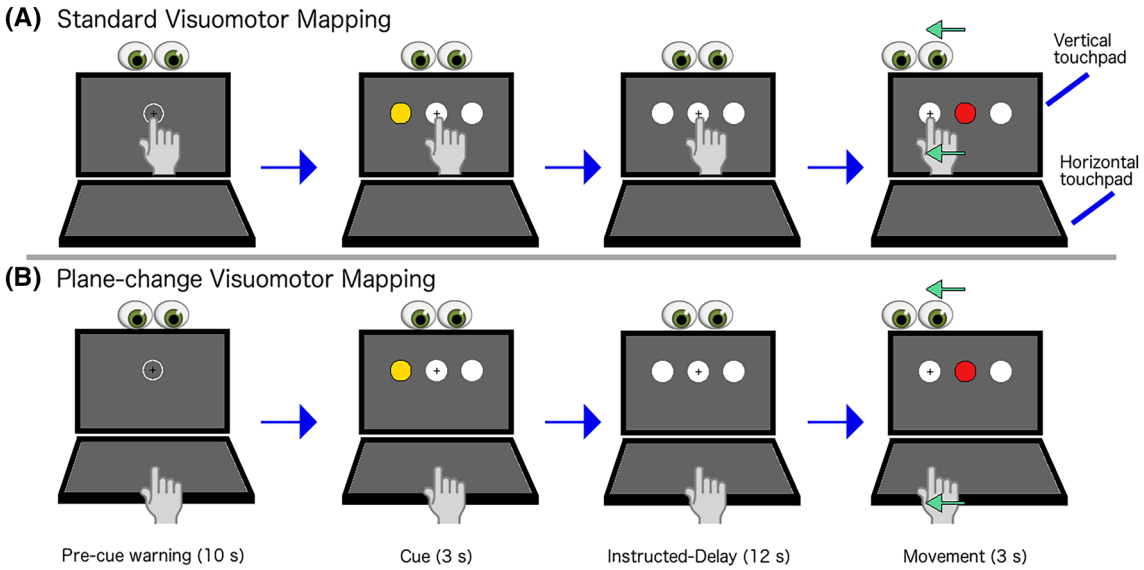

Fig. 1 Schematic representation of the standard and plane-change (non-standard) visuomotor mapping conditions. In both conditions, targets for movement were viewed on a vertical touch screen. Slow event-related trial structure required central fixation and the hand placed in a central position prior to a cue period, during the cue period (left or right peripheral target of interest turned yellow while the other target turned white), and during an instructed-delay period (both peripheral targets turned white). At the "go" signal (central target turned red) participants saccaded to the target that was yellow during the cue period. During the standard condition, they also slid their finger across the vertical touch screen to the location of the cued target. During the plane-change condition, participants slid their finger across the horizontal touch screen to move a cursor into the cued target

eye being partially blocked by the eyelid of most participants. However, the eye tracker data were reliable enough to verify fixation during times of the paradigm that required it and to verify that saccades were made towards the visual target rather than to the horizontal plane. These data were thus used solely to verify task compliance.

Experimental paradigm

Participants were trained on the experimental tasks prior to scanning. The experimenter demonstrated performance of the tasks prior to participants performing one full practice experimental run containing a block of each condition (described in detail, below). In addition, each participant was provided with an illustrated description of the tasks and MRI set-up several days prior to scanning. To limit task-related head movements, participants were instructed to make small, smooth arm movements using the wrist and elbow only rather than initiating movements as quickly as possible and these movements were practiced prior to scanning.

During MRI data collection, each participant performed four experimental runs. The start of each run was synchronized with the MRI pulse sequence using output from the MRI control computer to the computer running the stimulus presentation software. Each run contained two blocks (one per condition) of slow event-related trials. Blocks of each condition were presented in random order within an imaging run. Stimuli were back-projected onto the vertical touchpad. Each run began with 15 s of fixation on a central dot. Each block of trials in a condition began with the presentation of an instruction screen (6 s) informing the participant which experimental condition they would perform in the upcoming block of 9 trials. Instruction screens were followed by 15 s of central fixation. Inter-trial intervals (during which time participants fixated on a central dot) were also 15 s long in total; however, 5 s into each inter-trial interval, the fixation dot expanded into a hollow circle. This hollow circle provided the participant with a cue to move their hand from the resting position on their abdomen to the central position of the touchpad and then keep it still in preparation for the upcoming trial. At the start of each trial, there was a cue period (3 s) during which time the centre target (which the participant was fixating and touching) turned from a hollow white circle to a filled white circle with two circular targets appearing peripherally on the left and right (Fig. 2). Peripheral targets were positioned 70 mm away from the central target (centre-to-centre distance). The distance of the central target from the participant's eyes was approximately 500 mm but varied depending on the size of the participant and the exact head position in the head cradle. Therefore, the visual angle from central to peripheral targets was approximately 8°. During the cue period, one of the two peripheral targets (at random) was coloured yellow

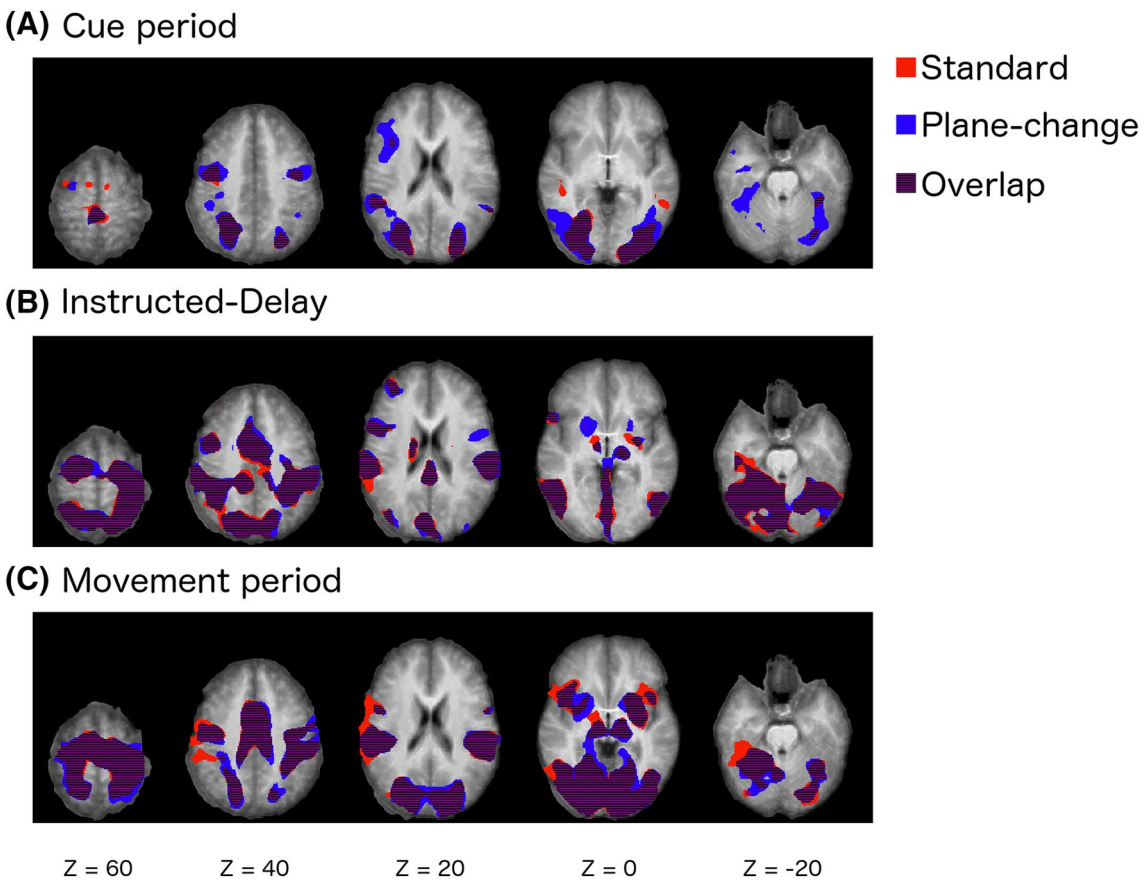

Fig. 2 Group mean activity associated with the standard condition (red), plane-change condition (blue), and overlap of activity associated with both conditions (patterned purple) relative to baseline fixation in **a** the cue period, **b** the instructed-delay period, and **c** the movement period for all trials. Thresholding for all epochs using FDR of $q < 0.01$. False colour overlays are shown on axial slices of the group mean anatomical image. Talairach z values are indicated below each slice

indicating that it was the target for movement for the trial. The other target of non-interest was a hollow white circle. Participants remained fixated on and touching the central target during the cue period. After the cue period, there was an instructed-delay period (12 s) where the yellow circle of the cued target became a hollow white circle identical to the non-cued target. The central target remained a filled white circle. Participants continued to fixate and touch the central target. After the delay period, a "go" signal was given in the form of the central target turning from white to red. This movement period lasted for 3 s. At the "go" signal, participants were required to move their gaze to the target that had been coloured yellow during the cue. The required hand movement differed depending on which experimental condition was being presented in a block. For the "Standard" visuomotor mapping condition, the hand was also required to slide along the vertical touchpad to the target that was cued (i.e. movements of the gaze and hand were spatially coupled). For the "Plane-change" (non-standard) condition, the hand was required to slide along the horizontal touchpad, moving a cursor on the vertical touchpad to the cued target (i.e. the hand movement was made on a different plane than the visual information guiding the movement). Note that the cursor was also visible in the standard condition but that it was partially occluded by the participant's fingertip. Each experimental run contained one block of each condition and each condition had nine trials. Trials for the left and right targets were presented at random but with equal numbers of trials in each direction presented in the two experimental conditions within each imaging run. Each participant performed 4 experimental runs giving a total of 36 trials for each of the two conditions.

Movements made in the two experimental conditions were kept as kinematically similar as possible while still allowing us to spatially dissociate arm movements from the guiding visual information. Depending on the size of the participant, there was an arm-postural difference of approximately 20° of increased elbow flexion and approximately 40° of increased wrist extension for movements made on the vertical screen relative to the horizontal screen. Shoulder position did not vary between conditions. Distances between the central and peripheral targets were equivalent on the two

screens. Movements were only made to either the left or right (rather than including targets above or below the central position which would have required upward and downward movements on the vertical screen but movements away and toward the participant on the horizontal screen). Therefore, despite slight postural differences, equal amounts of wrist and elbow deviation were required during arm movements made in both conditions.

Behavioural data

Analysis of eye and hand movements was performed using custom-written software in Matlab (The MathWorks Inc., Natick, MA, USA). Individual trials were considered successful and included in the data analysis if the eyes remained fixated throughout the trial until the "go" signal and then made a saccade in the correct direction. Similarly, the hand had to remain still on the touchpad until receiving the "go" signal and then had to move to the correct target without direction reversals. Trials containing movements that were not completed prior to the end of the movement period of a trial were discarded. However, inclusion criteria did not have specific reaction time (RT) or movement time (MT) thresholds because participants were encouraged to move slowly and smoothly to avoid creating task-related motion artifacts in the MRI data. RT was calculated as the time after the "go" signal at which the velocity of the hand on the touchpad first reached 10% of the peak ballistic velocity for the trial. Ballistic movement time (MTb) was calculated as the amount of time between RT and the timepoint when the velocity of the movement first decreased back down to 10% of the peak velocity. Corrected movement time (MTc) was calculated as the amount of time between the RT and the conclusion of any small corrective movements made after the first ballistic movement. Ballistic and corrected absolute errors (AEb and AEc) were calculated as the absolute distance between the average movement endpoint and the actual centre of the target. Ballistic and corrected variable errors (VEb and VEc) were calculated as the distance between the endpoints of movements of individual trials and the mean of these endpoint locations. Paired *t* tests were performed to compare variables between the two experimental conditions (i.e. movements made on the vertical and horizontal touchpads).

Preprocessing of MRI data

MRI data were analyzed using BrainVoyager QX (v2.8, and v20.6 Brain Innovation, Maastricht, The Netherlands). Head motion (translation and rotation) was viewed in real-time in the MRI control room to verify that head movement did not exceed 1 mm in any direction. One participant was required to repeat 1 experimental run due to excess head movement. Preprocessing of the data included motion correction using a trilinear/sinc interpolation algorithm with the volume closest to the time of the anatomical scan acquisition used as the reference volume. Plots and movies of head movement over time for each experimental run were generated by the analysis software and visually inspected to confirm that all runs included in the analysis were free from head movements over 1 mm and free from scanner-related artifacts. Data preprocessing also included slice time correction and linear trend removal. Experimental protocol design matrices were generated from each participant's stimulation protocol for each run (boxcar design) and convolved with a hemodynamic response function. Within each stimulation protocol, separate predictors were defined for cue periods, instructed-delay periods, and movement periods in each trial for each of the two experimental conditions. Predictors were also defined for the instruction periods preceding each of the two blocks of trials. Trials for the left and right targets were pooled together within each condition. In addition, individual head motion profiles in three linear and three rotational directions were added to each participant's stimulation protocols as predictors of non-interest.

Whole-brain recursive feature elimination multi-voxel pattern analysis (RFE MVPA)

Functional MRI data were normalized to Talairach space but spatial smoothing was not performed at this level of data preprocessing. Correction for signal intensity inhomogeneity was performed on T1-weighted images. Voxel intensity thresholding of each participant's T1-weighted anatomical image was used to create segmentation masks that included cortical and cerebellar grey matter. These grey matter masks were transformed from the spatial resolution of the anatomical image (i.e. 1 mm^3) to that of the functional images (i.e. 3 mm^3). Each participant's mask contained approximately 50,000 voxels.

For each trial (36 per condition), multi-voxel pattern response estimates were created for input into the classification algorithm. BOLD signal values for each voxel were *z*-normalized to remove any potential differences in the mean signal amplitudes associated with the two experimental conditions (Coutanche 2013). This approach was used to mean centre voxel responses to zero, preserving relative voxel BOLD signal amplitude differences but removing potential overall differences between the experimental conditions. To examine if pattern-based discrimination between conditions changed over the time-course of movement preparation and execution, three sets of trial estimates were extracted and were time-locked respectively to the cue, instructed-delay, and movement epochs of trials. Estimates were generated by fitting a general linear model with a predictor (cue, instructed-delay, or movement) using a boxcar design

convolved with a double-gamma hemodynamic response function. Resulting beta values at each voxel were divided by the standard error estimate at that voxel to obtain a *t* value. Use of *t* value estimates rather than beta weight estimates has been observed to suppress the contribution of voxels with high beta estimates due to high levels of noise (Misaki et al. 2010).

Voxel reduction was performed using a univariate activation-based approach to select the top 50% of voxels demonstrating task-related activity. This feature-selection method reduced grey matter masks to approximately 25,000 voxels. Limiting the RFE algorithm search space has been demonstrated to reduce the likelihood of over-fitting the classifier (Guyon and Elisseeff 2003) and to produce a more robust result from RFE analyses (De Martino et al. 2008).

Recursive feature elimination was performed using a linear support vector machine classifier (Coutanche 2013). RFE is a multivariate, iterative machine-learning algorithm for detecting patterns of voxel activity that are discriminative between categories in the absence of a priori hypotheses regarding the anatomical location of potential effects (Guyon and Elisseeff 2003; De Martino et al. 2008; Staeren et al. 2009). RFE uses a wrapper feature-selection strategy to localize a subset of voxels that maximize generalization of the linear SVM classifier. A step-wise voxel elimination is performed, where the weight magnitudes derived from the SVM classification are used as ranking criteria for selecting the most highly task-discriminative voxels. With each iteration of the algorithm, voxels that are most sensitive for category discrimination (i.e. have the highest SVM weights) are selected and then the classifier is re-trained using this reduced set of voxels in the next iteration. The final desired percentage of "surviving" voxels was specified at 20% of the total number of voxels originally input into the RFE process leaving approximately 5000 voxels for each participant.

Within the RFE process, two nested levels of cross-validation were performed. The first level of cross-validation was set to five folds and the SVM weight values for the final set of surviving voxels were derived from the mean results of these folds. Within each of these five folds of the first level of the cross-validation, a second-level cross-validation partitioned the trials into 50 splits for each of 10 gradual voxel elimination stages. The final set of voxels for each of these reductions were those with the highest mean absolute weights across all 50 splits. Ranking scores were spatially smoothed 2 mm using a full-width half-maximum filter prior to selection of voxels to favor the selection of clusters of voxels with significant SVM weight rankings rather than isolated voxels which can more easily achieve a high weighting by chance alone.

The SVM RFE process was performed separately for each participant and resulted in whole-brain weight maps (*w* value) of voxels discriminating between the two experimental conditions. Weight maps were converted to absolute values and then averaged to create mean group weight maps for the cue, instructed-delay, and movement epochs. The absolute value of a weight ranking in a voxel directly reflects the importance of that voxel in discriminating between the two tested conditions (i.e. classes) such that a higher value indicates greater discrimination between conditions. Voxels with low weight rankings are unlikely to persist in the group mean weight map unless they have achieved statistical significance in several individual participant weight maps. Weight values are scaled to a range of 0–10 during creation of weight maps. Group weight maps were thresholded at $w > 2.0$, reducing the likelihood that voxels obtaining significant SVM classification by chance alone would be included in the mean result. In addition, cluster thresholding of 20 consecutive voxels was applied to group maps. Finally, to ensure that the regions in which spatial patterns of discrimination were detected were consistent across participants, regions were only included if at least 8 of 10 participants' individual RFE maps contained at least 10 significantly discriminative voxels that overlapped with a region detected in the group mean map. The regions reported in group maps in Table 2 contain a mean value of approximately 211 voxels. Given that RFE for each participant was performed on masks containing approximately 25,000 starting voxels, the likelihood of the RFE procedure finding 10 surviving voxels in a reported region by chance alone is approximately 1.83×10^{-21} for a single participant, making the likelihood of this occurring in 80% of participants extremely low. Thus the regions reported within the group mean weight maps may be interpreted as containing spatial patterns of activity that are consistently discriminative between the two visuomotor conditions across the participants of the study (Staeren et al. 2009).

Whole-brain general linear model comparisons of visuomotor mapping conditions

Preprocessing of the data was done as above for the RFE analysis (i.e. motion correction, slice time correction and linear trend removal). In addition, the data were spatially smoothed 6 mm using a full-width half-maximum isotropic kernel. A random effects general linear model was performed using BrainVoyager v20.6. Contrasts of activity between the standard and plane-change visuomotor mapping conditions were performed for each trial epoch (i.e. cue, delay, and movement periods) using two-sample paired *t* tests implementing nonparametric permutation testing. For each contrast, 1000 permutations were run and a threshold-free cluster enhancement (TFCE) approach was used (Smith and Nichols 2009).

Results

Behavioural data

Ballistic absolute and variable errors were significantly higher in the plane-change condition than in the standard mapping condition (Table 1). However, after movement corrections, endpoint errors no longer differed between the tasks. There were no significant task-related differences in any of the timing variables (i.e. reaction time, movement time, or peak velocity). Numbers of errors made (i.e. failure to move, movement at the wrong time, or in the wrong direction, etc.) were very low with the majority of participants making zero errors. One participant made 2 errors in each of the two visuomotor conditions. These four trials were removed from further analysis.

Whole-brain general linear model comparisons of visuomotor mapping conditions

Contrasts of BOLD signal amplitude comparing the standard and plane-change conditions did not reveal any significant differences in any region of the brain. Figure 2 demonstrates extensive overlap in the group mean patterns of activity for the Standard and Plane-change conditions relative to baseline activity for each of the three trial epochs (i.e. cue, instructed-delay, and motor execution).

Whole-brain recursive feature elimination multi-voxel pattern analysis (RFE MVPA)

The group mean classification accuracy across the brain over the two visuomotor mapping conditions was calculated using the final cross-validation fold from each participant (Fig. 3). Discrimination between the two conditions progressively increased over the three epochs (i.e. cue, instructed-delay, and motor execution) with mean classification accuracy significantly higher in each time period, indicating increasingly different patterns of brain activity associated with the two conditions from the planning stages through to movement. Similarly, the number of voxels found to decode the two conditions across the group of participants increased dramatically in each epoch with 250 voxels in the cue period, 1263 voxels in the instructed-delay period, and 2704 voxels in the motor execution period. Descriptions of regions in which discrimination between the two tasks occurred are shown in Table 2. These regions are also shown overlaid on a Talairach-normalized brain from one participant in Fig. 4.

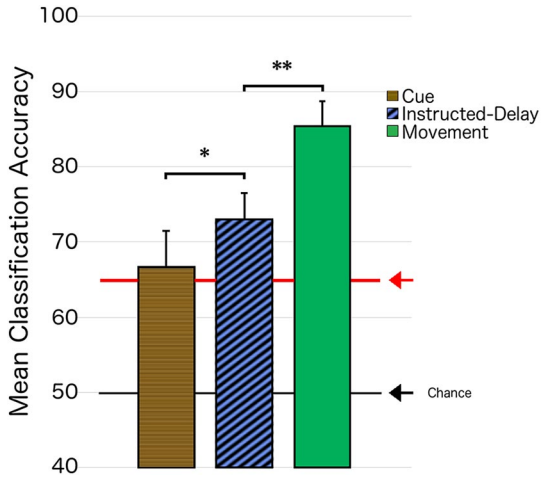

Fig. 3 Group mean accuracy of visuomotor task classification for the final cross-validation fold of whole-brain recursive feature elimination multi-voxel pattern analysis during the cue, instructed-delay, and motor execution epochs. Error bars represent standard error of the mean. * represents paired *t* test *p* value < 0.05 and ** represents *p* value < 0.01

Table 1 Mean values of kinematic variables for the two visuomotor mapping conditions

	Standard visuomotor mapping (± SD)	Plane-change visuomotor mapping (± SD)	Paired *t* test *p* value
Reaction time (ms)	619 (± 141)	602 (± 119)	0.60
Ballistic movement time (ms)	1460 (± 406)	1487 (± 431)	0.62
Corrected movement time (ms)	1656 (± 458)	1756 (± 425)	0.11
Peak velocity (cm/s)	11.7 (± 2.0)	11.5 (± 1.7)	0.55
Ballistic absolute error (mm)	**11.7 (± 4.2)**	**15.0 (± 5.5)**	**0.012***
Corrected absolute error (mm)	9.1 (± 4.5)	9.4 (± 5.6)	0.68
Ballistic variable error (mm)	**12.0 (± 4.1)**	**16.1 (± 4.1)**	**0.026***
Corrected variable error (mm)	10.0 (± 4.7)	10.4 (± 5.7)	0.62

Bold values represent measures that were significantly different between the two visuomotor conditions

Asterisk represents *p*-value < 0.05

Table 2 Regions significantly decoding the standard and plane-change conditions in whole-brain recursive feature elimination MVPA for the cue, instructed-delay, and movement execution periods

Region (Brodmann area designation of centre of gravity)	Mean $X \pm$ SD	Mean $Y \pm$ SD	Mean $Z \pm$ SD	#Voxels (3 mm^3)
Cue period				
R. middle frontal gyrus (BA 10)	37 ± 5	47 ± 5	6 ± 4	65
L. precuneus (BA 7, extending into R. precuneus)	−2 ± 5	−45 ± 10	46 ± 10	185
Instructed-delay period				
L. medial frontal gyrus (BA 10)	−9 ± 4	48 ± 4	10 ± 9	85
R. medial premotor (BA 6, extending into L. medial premotor)	3 ± 6	−10 ± 14	57 ± 14	289
L. lateral premotor (BA 6)	−20 ± 6	−18 ± 8	61 ± 5	88
R. insula (BA 6 extending into BA 13)	45 ± 11	−1 ± 9	10 ± 6	164
R. primary motor (BA 4)	28 ± 9	−23 ± 7	57 ± 6	191
L. lingual gyrus (BA 18, extending into cuneus)	−12 ± 7	−82 ± 10	1 ± 9	327
R. lingual gyrus (BA 18, extending into cuneus)	16 ± 7	−89 ± 5	6 ± 7	119
Movement period				
R. medial premotor (BA6, extending into L. medial premotor)	4 ± 4	2 ± 8	46 ± 6	122
L. primary motor (BA4, extending into primary somatosensory and lateral premotor)	−32 ± 10	−26 ± 11	54 ± 8	647
R. lateral premotor (BA 6)	14 ± 6	−2 ± 4	60 ± 4	86
R. superior parietal lobule (BA 7)	19 ± 7	−45 ± 6	59 ± 4	108
R. inferior parietal lobule (BA 40)	56 ± 4	−30 ± 5	27 ± 6	119
L. middle occipital gyrus (BA 19)	−42 ± 4	−71 ± 6	−2 ± 10	120
R. usiform gyrus (BA 37, extending into middle occipital gyrus)	46 ± 6	−60 ± 8	−2 ± 10	266
L. lingual gyrus (BA 18, extending into cuneus)	−8 ± 6	−76 ± 11	6 ± 14	592
R. lingual gyrus (BA 18, extending into cuneus)	7 ± 5	−76 ± 10	4 ± 12	562
L. cerebellum, anterior lobe	−39 ± 4	−52 ± 5	−20 ± 3	40
R. cerebellum, anterior lobe	23 ± 4	−45 ± 4	−16 ± 5	42

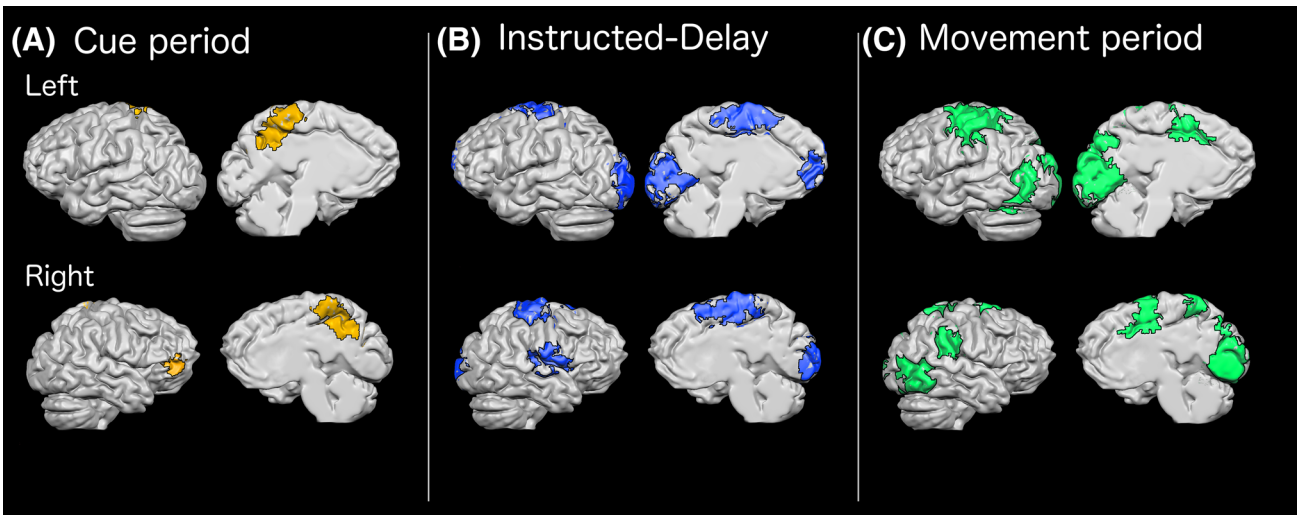

Fig. 4 Results of group whole-brain recursive feature elimination multi-voxel pattern analysis. Coloured regions represent voxels in which significant decoding of the standard versus plane-change visuomotor mapping conditions occurred during **a** the cue period (yellow), **b** the instructed-delay period (blue), and **c** the movement period (green). Regions are shown overlaid on a Talairach-normalized brain from one participant. Within each panel, the left hemisphere is shown at the top and the right hemisphere is shown on the bottom. Lateral surfaces are shown on the left of each panel and medial surfaces on the right

Discussion

Summary of main findings

During standard visually guided arm movements, the eyes and arm move to the same spatial location. In contrast, non-standard visuomotor mappings introduce a spatial dissociation between the targets of saccadic and reaching movements. In the current study, we used fMRI to compare brain activity between standard reaching movements and a non-standard visuomotor mapping where arm movements were made in a different spatial plane relative to the guiding visual information. This comparison allowed us to examine the neural correlates of dissociating the proprioceptive and motoric components of movement production from visual input (sensorimotor recalibration), and to compare this pattern of activity directly to standard eye–hand coordination. Examinations of activity associated with the two conditions (i.e. Standard and Plane-change) relative to baseline activity demonstrated a great deal of overlap, suggesting that the two visuomotor mapping conditions evoked activity in similar regions of the brain. Statistically contrasting the amplitude of the BOLD fMRI signal between the two conditions did not reveal significant differences in amounts of activity in any location in the brain. However, use of a whole-brain multivoxel approach revealed multiple regions where the spatial patterns of voxel activity differentiated the two tasks, suggesting that the nature of activity within some of the commonly activated regions differed depending on visuomotor mapping even if overall amounts of activity were similar. In addition, this analysis revealed that as movement preparation progressed toward motor execution, successful decoding of the two visuomotor conditions became progressively more accurate and involved progressively more brain regions. Specifically, production of a standard visually guided arm movement and production of a non-standard arm movement requiring implicit sensorimotor recalibration relied on similar patterns of brain activity during the initial stages of movement preparation. Progressively discernable patterns of brain activity evolved as motor execution approached, culminating in discriminable patterns of activity throughout areas involved in visually guided reaching movements, including frontal, parietal, occipital, and cerebellar regions.

Differences in intermediate accuracy and precision prior to final movement corrections

The use of a slow event-related trial structure in this study allowed us to examine the time-course of brain activity during cue presentation, an instructed preparatory delay, and motor execution epochs. A whole-brain multi-voxel pattern analysis approach detected spatial patterns of voxel activity in several regions that discriminated between the two visuomotor mapping conditions. Differences in task proficiency are unlikely to account for the observed differences in patterns of brain activity. All participants reported extensive use of desktop computers, suggesting that the configuration of the non-standard task (i.e. looking at visual stimuli on a vertical screen and responding with movements on a horizontal plane) was familiar to all participants. Further, numbers of errors (such as moving in the wrong direction or at the wrong time) did not significantly differ between the two conditions and were very low overall, with the majority of participants making no errors. Reaction times, movement times, and peak velocities did not differ between the two conditions. Interestingly, ballistic accuracy and precision of hand movements were significantly lower in the non-standard task; however, after final movement corrections, these values were no longer significantly different. Though similar movement outcomes were achieved in both tasks, differences in intermediate accuracy and precision could represent a behavioural correlate of the observed differences in brain activity and are likely a consequence of spatially dissociating eye and arm movements.

Task discrimination increases as movement planning progresses toward movement execution

The number of voxels demonstrating significant decoding of the two visuomotor mapping tasks dramatically increased (by a factor of 5) from the cue period to the instructed-delay period and then approximately doubled again after the "go" signal for motor execution. This result suggests that as trials progressed toward movement execution, patterns of activity differed depending on the visuomotor task within an increasing number of brain regions. Mean accuracies of the classifier were also progressively higher during each of these periods, ranging from borderline significance during the cue period to increasingly higher significance during the delay and motor execution periods. This result suggests that as trials progressed toward movement execution, the level of distinctiveness of the activity patterns associated with each task also increased. Together, these observations demonstrate that spatial patterns of activity became progressively more discriminable in a growing number of brain regions as the visuomotor transformations proceeded through planning to movement execution.

The lack of regions discriminating between the two conditions early in movement planning (only the anterior prefrontal cortex and the precuneus) is notable. One possible explanation for this observation could be that the brain

initially plans movements for both sensorimotor mappings prior to choosing one for execution. Initial co-activation of patterns of activity associated with both mappings would produce largely indiscriminable overall patterns of voxel activity. Others have reported that when two potential targets for an arm movement appear, cells in the dorsal premotor cortex (PMd) with preferred directions matching either of the targets will discharge (Cisek and Kalaska 2005; Coallier et al. 2015). This finding suggests that when more than one potential movement is available, rather than selecting one target, the brain simultaneously plans responses to both targets. This co-activation of two neuronal populations, each coding one of two movement possibilities remains until a decision to move to one of the targets has been made. At this time, activity associated with movement toward the non-selected target is inhibited and only the population of neurons selective for the chosen target remain active. Other examples of simultaneous planning of multiple potential movements in the brain include the simultaneous activation of multiple cell populations observed in association with a reach target and distractor targets (Song and McPeek 2010) and for the targets of a sequence of movements (Medendorp et al. 2006). These findings suggest that rather than planning movements toward a single target, the brain plans movements to all potential targets prior to final selection. The progressive decoding we observed over trials in our tasks could be analogous to these demonstrations that the brain computes all potential motor possibilities. In other words, it is possible that the brain simultaneously plans reaches using both potential visuomotor mappings (i.e. the standard and plane-dissociated mappings) until a selection has to be made nearing the "go" signal. If concurrent planning of all potentially applicable visuomotor mappings occurs, one would expect patterns of activity representing both potential mappings to co-exist early in a trial. This possibility could account for the observed relative absence of multi-voxel decoding during the cue period, when motor planning regions might contain patterns of activity representing both mappings. Then as one of the potential visuomotor mappings was selected, one would expect inhibition of the non-selected mapping representation to leave only a pattern of activity associated with the chosen mapping and a corresponding increase in discriminative spatial patterns of voxel activity, as we observed during the instructed-delay period and then even more strongly in association with motor execution. In accord with this hypothesis, Klaes et al. (2011) recently reported that when a monkey has been trained to perform two different visuomotor mappings in association with a single visual cue (a standard mapping or a visuomotor rotation), cells in the premotor and parietal cortices display neural signals correlating to both of the two mappings until a decision is made at motor execution. Similarly, monkeys performing a comparable plane-change task as the present study (Hawkins et al. 2013) showed reduced activity in parietal area PEc (a putative homologue to human precuneus; Filimon et al. 2009) only during movement and target hold epochs, but not during the cue period. The findings presented in the current study may support the idea that when the actions triggered by a visual stimulus are context-dependent, the brain plans potential movements for all of the possible rules before choosing an action.

While some regions of the brain may simultaneously encode multiple potential motor outcomes, others must be involved in the final selection of a response that fits the context of the task. The prefrontal cortex is thought to be integral in representation of rules and their selection for producing an appropriate movement given multiple possibilities (Miller and Cohen 2001; Wallis and Miller 2003; Genovesio et al. 2005; Rowe et al. 2008). Prior to motor execution (i.e. during the cue and instructed-delay periods), voxels discriminating between the two visuomotor conditions were detected in the anterior prefrontal cortex (Brodmann area 10). This region has been previously reported in association with production of non-standard visuomotor mappings (Granek et al. 2010). In particular, greater activity in this region during non-standard movement production was associated with more time spent playing video games (which require non-standard mapping), suggesting that experience with non-standard movements influences processing in this region of the brain. Activity in the prefrontal cortex is thought to represent context-related rules and the goals of a response and that these regions configure downstream neural pathways to ensure motor execution appropriately reflects the context of a task (Miller and Cohen 2001). Our observation of discriminative voxels in the anterior prefrontal cortex during motor planning but not during execution suggests that this region may have been involved in choosing between the two potential visuomotor mapping responses prior to initializing a response.

Interestingly, in addition to early decoding of condition in the cue period in the anterior prefrontal cortex, strong bilateral decoding in the precuneus was also observed during this time period. Pellijeff and colleagues (Pellijeff et al. 2006) used fMRI to examine postural representations of the arm during non-visually guided, point-to-point arm movements made from various starting postures of the arm and only observed an effect in the precuneus. In the current study, examining the effects of spatially dissociating eye and arm movements relative to standard visuomotor mapping necessitated that the kinematic properties of arm movements differed between the two conditions (i.e. movements made on either the vertical or horizontal touch screens). Despite this requirement, movements in the two visuomotor mapping conditions were kept as similar as possible. In both cases, movements required either sliding the finger to the left or right (up and down/backward and

forward movements were not made). These movements were accomplished with small deflections at the wrist and elbow joints that did not differ in amplitude between the two conditions. The upper arm was made immobile using a strap and padding so the position of the shoulder joint did not differ between the two conditions. The arm position relative to the midline also did not differ between the conditions. However, there was a postural difference of approximately 20° of increased elbow flexion and approximately 40° of increased wrist extension for movements made on the vertical screen compared with the horizontal screen. Given the findings of others that activity in the precuneus is associated with arm posture in humans (Pellijeff et al. 2006), and similar findings in the superior parietal lobule of non-human primates (Kalaska and Hyde 1985; Scott et al. 1997), the early decoding of the standard and non-standard conditions in this region could provide further support for the idea that this region is involved in integrating starting arm position into the planning of goal-directed reaching movements.

Implicit versus explicit aspects of non-standard sensorimotor mapping

The results of behavioural sensorimotor adaptation studies have suggested that distinct neurological processes exist for explicit versus implicit sensorimotor recalibration (Smith et al. 2006; Taylor et al. 2014; McDougle et al. 2015). In a previous study we demonstrated that relative to standard visuomotor mapping, incorporation of an explicit rule—in this case, a visuomotor rotation—resulted in greater activity within the right inferior parietal lobule and the left superior posterior cerebellum (Gorbet and Sergio 2016). Further, multi-voxel pattern analysis revealed distinctive patterns of activity bilaterally within the medial premotor and cuneus regions. This previous study focused on the instructed-delay portion of trials. In contrast, when looking at the comparable instructed-delay epoch in the current study which involved an implicit sensorimotor recalibration (i.e. the plane-change), the GLM whole-brain comparison of activity level did not find activity differences in any region relative to the standard visuomotor mapping. When comparing the results of multi-voxel pattern analysis between the two studies, it is apparent that distinct patterns of activity occur in a greater number of brain regions in the current study; however, these areas include the bilateral medial premotor and cuneus regions that were seen with the visuomotor rotation task used in the previous study. Thus, these results suggest that the implicit and explicit components of non-standard mappings recruit different but partially overlapping neural substrates.

Conclusions

The study presented here demonstrates that when compared with standard visuomotor mapping, even a small spatial dissociation between guiding visual information and a motor response results in highly discriminable patterns of activity throughout visuomotor regions of the brain. These differences in brain activity become progressively more prominent as the visually guided response progresses through motor planning toward movement. Care should be taken to acknowledge the potential influence of non-standard visuomotor mapping on the results of studies of eye–hand coordination.

Funding The funding was received by Natural Sciences and Engineering Research Council of Canada (NSERC) (Grant no. 227220-2011).

Compliance with ethical standards

Conflict of interest The authors declare that they have no conflict of interest.

References

Batista AP, Buneo CA, Snyder LH, Andersen RA (1999) Reach plans in eye-centered coordinates. Science 285:257–260. https://doi.org/10.1126/science.285.5425.257

Bock O, Girgenrath M (2006) Relationship between sensorimotor adaptation and cognitive functions in younger and older subjects. Exp Brain Res Hirnforschung Exp Cerebrale 169:400–406. https://doi.org/10.1007/s00221-005-0153-4

Brown J, Dalecki M, Hughes C et al (2015) Cognitive-motor integration deficits in young adult athletes following concussion. BMC Sports Sci Med Rehabilit 7:1. https://doi.org/10.1186/s13102-015-0019-4

Buneo CA, Batista AP, Jarvis MR, Andersen RA (2008) Time-invariant reference frames for parietal reach activity. Exp Brain Res 188:77–89. https://doi.org/10.1007/s00221-008-1340-x

Buxbaum LJ, Coslett HB (1997) Subtypes of optic ataxia: reframing the disconnection account. Neurocase 3:159–166. https://doi.org/10.1093/neucas/3.3.159

Carey DP, Coleman RJ, Della Sala S (1997) Magnetic misreaching. Cortex 33:639–652

Chen Y, Monaco S, Byrne P et al (2014) Allocentric versus egocentric representation of remembered reach targets in human cortex. J Neurosci 34:12515–12526. https://doi.org/10.1523/JNEUROSCI.1445-14.2014

Cisek P, Kalaska JF (2005) Neural correlates of reaching decisions in dorsal premotor cortex: specification of multiple direction choices and final selection of action. Neuron 45:801–814. https://doi.org/10.1016/j.neuron.2005.01.027

Coallier É, Michelet T, Kalaska JF (2015) Dorsal premotor cortex: neural correlates of reach target decisions based on a color-location matching rule and conflicting sensory evidence. J Neurophysiol 113:3543–3573. https://doi.org/10.1152/jn.00166.2014

Cohen YE, Andersen RA (2002) A common reference frame for movement plans in the posterior parietal cortex. Nat Rev 3:553–562. https://doi.org/10.1038/nrn873

Coutanche MN (2013) Distinguishing multi-voxel patterns and mean activation: why, how, and what does it tell us? Cogn Affect Behav Neurosci 13:667–673. https://doi.org/10.3758/s13415-013-0186-2

Crawford JD, Medendorp WP, Marotta JJ (2004) Spatial transformations for eye–hand coordination. J Neurophysiol 92:10–19. https://doi.org/10.1152/jn.00117.2004

Dalecki M, Albines D, Macpherson A, Sergio LE (2016) Prolonged cognitive–motor impairments in children and adolescents with a history of concussion. Concussion. https://doi.org/10.2217/cnc-2016-0001

De Martino F, Valente G, Staeren N et al (2008) Combining multivariate voxel selection and support vector machines for mapping and classification of fMRI spatial patterns. Neuroimage 43:44–58. https://doi.org/10.1016/j.neuroimage.2008.06.037

Filimon F, Nelson JD, Huang RS, Sereno MI (2009) Multiple parietal reach regions in humans: cortical representations for visual and proprioceptive feedback during on-line reaching. J Neurosci 29:2961–2971. https://doi.org/10.1523/JNEUROSCI.3211-08.2009

Fisk JD, Goodale MA (1985) The organization of eye and limb movements during unrestricted reaching to targets in contralateral and ipsilateral visual space. Exp Brain Res 60:159–178. https://doi.org/10.1007/BF00237028

Frassinetti F, Bonifazi S, Làdavas E (2007) The influence of spatial coordinates in a case of an optic ataxia-like syndrome following cerebellar and thalamic lesion. Cogn Neuropsychol 24:324–337. https://doi.org/10.1080/02643290701275857

Genovesio A, Brasted PJ, Mitz AR, Wise SP (2005) Prefrontal cortex activity related to abstract response strategies. Neuron 47:307–320. https://doi.org/10.1016/j.neuron.2005.06.006

Gorbet DJ, Sergio LE (2007) Preliminary sex differences in human cortical BOLD fMRI activity during the preparation of increasingly complex visually guided movements. Eur J Neurosci 25:1228–1239. https://doi.org/10.1111/j.1460-9568.2007.05358.x

Gorbet DJ, Sergio LE (2016) Don't watch where you're going: the neural correlates of decoupling eye and arm movements. Behav Brain Res. https://doi.org/10.1016/j.bbr.2015.11.012

Gorbet DJ, Staines WR (2011) Inhibition of contralateral premotor cortex delays visually guided reaching movements in men but not in women. Exp Brain Res 212:315–325. https://doi.org/10.1007/s00221-011-2731-y

Gorbet DJ, Staines WR, Sergio LE (2004) Brain mechanisms for preparing increasingly complex sensory to motor transformations. Neuroimage 23:1100–1111. https://doi.org/10.1016/j.neuroimage.2004.07.043

Gorbet DJ, Mader LB, Richard Staines W (2010) Sex-related differences in the hemispheric laterality of slow cortical potentials during the preparation of visually guided movements. Exp Brain Res 202:633–646. https://doi.org/10.1007/s00221-010-2170-1

Granek JA, Sergio LE (2015) Evidence for distinct brain networks in the control of rule-based motor behavior. J Neurophysiol 114:1298–1309. https://doi.org/10.1152/jn.00233.2014

Granek JA, Gorbet DJ, Sergio LE (2010) Extensive video-game experience alters cortical networks for complex visuomotor transformations. Cortex 46:1165–1177. https://doi.org/10.1016/j.cortex.2009.10.009

Granek J, Pisella L, Stemberger J et al (2013) Decoupled visually-guided reaching in optic ataxia: differences in motor control between canonical and non-canonical orientations in space. PLoS One 8:1–18. https://doi.org/10.1371/journal.pone.0086138

Grigorova V, Bock O, Ilieva M, Schmitz G (2013) Directional adaptation of reactive saccades and hand pointing movements is not independent. J Mot Behav 45:101–106. https://doi.org/10.1080/00222895.2012.750590

Guyon I, Elisseeff A (2003) An introduction to variable and feature selection. J Mach Learn Res 3:1157–1182

Hawkins KM, Sergio LE (2014) Visuomotor impairments in older adults at increased Alzheimer's disease risk. J Alzheimers Dis 42:607–621. https://doi.org/10.3233/JAD-140051

Hawkins KM, Sayegh P, Yan X et al (2013) Neural activity in superior parietal cortex during rule-based visual-motor transformations. J Cogn Neurosci 25:436–454. https://doi.org/10.1162/jocn_a_00318

Hawkins KM, Goyal AI, Sergio LE (2015) Diffusion tensor imaging correlates of cognitive-motor decline in normal aging and increased Alzheimer's disease risk. J Alzheimer's Dis. https://doi.org/10.3233/JAD-142079

Henriques DY, Cressman EK (2012) Visuomotor adaptation and proprioceptive recalibration. J Mot Behav 44:435–444. https://doi.org/10.1080/00222895.2012.659232

Heuer H, Hegele M (2011) Generalization of implicit and explicit adjustments to visuomotor rotations across the workspace in younger and older adults. J Neurophysiol 106:2078–2085. https://doi.org/10.1152/jn.00043.2011

Hurtubise J, Gorbet D, Hamandi Y et al (2016) The effect of concussion history on cognitive-motor integration in elite hockey players. Concussion 1:CNC17. https://doi.org/10.2217/cnc-2016-0006

Kalaska JF, Hyde ML (1985) Area 4 and area 5: differences between the load direction-dependent discharge variability of cells during active postural fixation. Exp Brain Res 59:197–202

Klaes C, Westendorff S, Chakrabarti S, Gail A (2011) Choosing goals, not rules: deciding among rule-based action plans. Neuron 70:536–548. https://doi.org/10.1016/j.neuron.2011.02.053

Kröller J, De Graaf JB, Prablanc C, Pélisson D (1999) Effects of short term adaptation of saccadic gaze amplitude on hand-pointing movements. Exp Brain Res 124:351–362. https://doi.org/10.1007/s002210050632

Lee D, Poizner H, Corcos DM, Henriques DY (2014) Unconstrained reaching modulates eye–hand coupling. Exp Brain Res 232:211–223. https://doi.org/10.1007/s00221-013-3732-9

McDougle SD, Bond KM, Taylor JA (2015) Explicit and implicit processes constitute the fast and slow processes of sensorimotor learning. J Neurosci 35:9568–9579. https://doi.org/10.1523/JNEUROSCI.5061-14.2015

McNay EC, Willingham DB (1998) Deficit in learning of a motor skill requiring strategy, but not of perceptuomotor recalibration, with aging. Learn Mem 4:411–420

Medendorp WP, Goltz HC, Vilis T (2006) Directional selectivity of BOLD activity in human posterior parietal cortex for memory-guided double-step saccades. J Neurophysiol 95:1645–1655. https://doi.org/10.1152/jn.00905.2005

Miller EK, Cohen JD (2001) An integrative theory of prefrontal cortex function. Annu Rev Neurosci 24:167–202. https://doi.org/10.1146/annurev.neuro.24.1.167

Misaki M, Kim Y, Bandettini PA, Kriegeskorte N (2010) Comparison of multivariate classifiers and response normalizations for pattern-information fMRI. Neuroimage 53:103–118. https://doi.org/10.1016/j.neuroimage.2010.05.051

Mushiake H, Fujii N, Tanji J (1996) Visually guided saccade versus eye-hand reach: contrasting neuronal activity in the cortical supplementary and frontal eye fields. J Neurophysiol 75:2187–2191

Neggers SF, Bekkering H (2000) Gaze anchoring to a pointing target is present during the entire pointing movement and is driven by a non-visual signal. J Neurophysiol 83:961–970

Pellijeff A, Bonilha L, Morgan PS et al (2006) Parietal updating of limb posture: an event-related fMRI study. Neuropsychologia 44:2685

Prablanc C, Echallier JF, Komilis E, Jeannerod M (1979) Optimal response of eye and hand motor systems in pointing at a visual target. I. Spatio-temporal characteristics of eye and hand movements and their relationships when varying the amount of visual information. Biol Cybern 35:113–124

Redding GM, Wallace B (1993) Adaptive coordination and alignment of eye and hand. J Mot Behav 25:75–88. https://doi.org/10.1080/00222895.1993.9941642

Reyes-Puerta V, Philipp R, Lindner W, Hoffmann K-P (2010) Role of the rostral superior colliculus in gaze anchoring during reach movements. J Neurophysiol 103:3153–3166. https://doi.org/10.1152/jn.00989.2009

Rowe J, Hughes L, Eckstein D, Owen AM (2008) Rule-selection and action-selection have a shared neuroanatomical basis in the human prefrontal and parietal cortex. Cereb Cortex 18:2275–2285. https://doi.org/10.1093/cercor/bhm249

Salek Y, Anderson ND, Sergio L (2011) Mild cognitive impairment is associated with impaired visual-motor planning when visual stimuli and actions are incongruent. Eur Neurol 66:283–293

Sayegh PF, Hawkins KM, Hoffman KL, Sergio LE (2013) Differences in spectral profiles between rostral and caudal premotor cortex when hand-eye actions are decoupled. J Neurophysiol 110:952–963. https://doi.org/10.1152/jn.00764.2012

Sayegh PF, Hawkins KM, Neagu B et al (2014) Decoupling the actions of the eyes from the hand alters beta and gamma synchrony within SPL. J Neurophysiol. https://doi.org/10.1152/jn.00793.2013

Sayegh PF, Gorbet DJ, Hawkins KM et al (2017) The contribution of different cortical regions to the control of spatially decoupled eye–hand coordination. J Cogn Neurosci 29:1194–1211. https://doi.org/10.1162/jocn_a_01111

Scott SH, Sergio LE, Kalaska JF (1997) Reaching movements with similar hand paths but different arm orientations. II. Activity of individual cells in dorsal premotor cortex and parietal area 5. J Neurophysiol 78:2413–2426

Smith S, Nichols T (2009) Threshold-free cluster enhancement: addressing problems of smoothing, threshold dependence and localisation in cluter inference. Neuroimage 44:83–98

Smith MA, Ghazizadeh A, Shadmehr R (2006) Interacting adaptive processes with different timescales underlie short-term motor learning. PLoS Biol 4:1035–1043. https://doi.org/10.1063/1.2184639

Snyder LH, Batista AP, Andersen RA (2000) Saccade-related activity in the parietal reach region. J Neurophysiol 83:1099–1102. https://doi.org/10.1152/jn.2000.83.2.1099

Song J-H, McPeek RM (2010) Roles of narrow- and broad-spiking dorsal premotor area neurons in reach target selection and movement production. J Neurophysiol 103:2124–2138. https://doi.org/10.1152/jn.00238.2009

Staeren N, Renvall H, De Martino F et al (2009) Sound categories are represented as distributed patterns in the human auditory cortex. Curr Biol 19:498–502. https://doi.org/10.1016/j.cub.2009.01.066

Taylor JA, Krakauer JW, Ivry RB (2014) Explicit and implicit contributions to learning in a sensorimotor adaptation task. J Neurosci 34:3023–3032. https://doi.org/10.1523/JNEUROSCI.3619-13.2014

Tippett WJ, Sergio LE (2006) Visuomotor integration is impaired in early stage Alzheimer's disease. Brain Res 1102:92–102. https://doi.org/10.1016/j.brainres.2006.04.049

Tippett WJ, Sergio LE, Black SE (2012) Compromised visually guided motor control in individuals with Alzheimer's disease: can reliable distinctions be observed? J Clin Neurosci 19:655–660. https://doi.org/10.1016/j.jocn.2011.09.013

Wallis JD, Miller EK (2003) From rule to response: neuronal processes in the premotor and prefrontal cortex. J Neurophysiol 90:1790–1806. https://doi.org/10.1152/jn.00086.2003

Wise SP, di Pellegrino G, Boussaoud D (1996) The premotor cortex and nonstandard sensorimotor mapping. Can J Physiol Pharmacol 74:469–482